



Visible light-induced selective oxidation of alcohols with air by dye-sensitized TiO₂ photocatalysis



Xia Li^a, Ji-Long Shi^a, Huimin Hao^a, Xianjun Lang^{a,b,*}

^a College of Chemistry and Molecular Sciences, Wuhan University, Wuhan 430072, China

^b Key Laboratory of Advanced Energy Materials Chemistry (Ministry of Education), Nankai University, Tianjin 300071, China

ARTICLE INFO

Keywords:

Heterogeneous photocatalysis
Alizarin red S
Titanium dioxide
Atmosphere oxygen
Oxidation of alcohol

ABSTRACT

Visible light-induced selective oxidation of alcohols to aldehydes or ketones with atmosphere oxygen was triumphantly achieved devoid of any redox mediator. A paradigm of dye-sensitized TiO₂ photocatalysis was capable of animating selective oxidation of a myriad of alcohols by 0.67 mol% of alizarin red S anchored onto TiO₂ surface under the irradiation of green light-emitting diodes. In essence, both a robust dye like ARS and anatase TiO₂ with a high specific surface area hold the key to unlock the high photocatalytic activity; and superoxide is pivotal in affording the selective oxidation product. This discovery could shed light on the design of visible light photocatalysis for selective organic transformations under ambient conditions by harvesting the cooperation between an organic dye and a metal oxide.

1. Introduction

Heterogeneous photocatalysis has been under intensive investigations for several decades due to its pertinence in the production of renewable energy and remediation of a polluted environment [1–3]. In these applications, it has been commonly associated with non-selective free radical reaction pathways. Simple inorganic molecules like H₂ or CO₂ is the final product for the photocatalytic reduction or oxidation of organic compounds. Therefore, the potential of heterogeneous photocatalysis in selective redox transformation was not well exploited in which the functionalized organic molecules are the end products, relying heavily on more precise control of reactive oxygen species (ROS). Recently, the unravelling of new mechanistic pathways [4] and the discovery of new photocatalytic materials [5] enable heterogeneous photocatalysis to become a powerful tool for selective organic transformations in an environmentally friendly manner [6–9]. In this development, the redox conversions of hetero-atom containing organic compounds has been widely studied amongst which the photocatalytic selective oxidation reactions with O₂ was more difficult than the reduction reactions [10,11]. In particular, the selective oxidation of alcohols is proven more challenging than the other compounds due to the relative inertness of the C_α-H bond next to an O-atom. Therefore, this reaction turns out to be the most popular probe reaction for verifying the photo-induced ability of new materials under ultraviolet (UV) or visible light irradiation.

Conventional metal oxide photocatalysts such as TiO₂ [12], ZnO

[13], Nb₂O₅ [14], TiO₂-WO₃ [15], BiWO₆ [16] or Bi₂MoO₆ [17] for the selective oxidation of alcohols with O₂ require the irradiation of UV light to overcome the large bandgaps of these semiconducting materials, leading to charge separation and the subsequent oxidation reactions. In addition, TiO₂-based composites were also applied into the selective oxidation of alcohols under UV irradiation [18]. Visible light photocatalysis can offer a more efficient way for conversion of solar energy and deliver the desired results for the selective oxidation of alcohols with O₂. In response, much effort was focused on this direction of research. One key development is based on the discovery of visible light active new materials. Four types of newly discovered materials like supported plasmonic metal or noble metal nanoparticles [19–22], metal organic frameworks (MOFs) [23,24], porous organic polymers (POPs) [25,26] and metal oxides like Bi₂WO₆ [27], Bi₂MoO₆ [28], BiVO₄ [29,30] and TiO₂ [31,32] have been submitted to the visible light photocatalytic selective aerobic oxidation of alcohols with considerable success. However, plasmonic nanoparticles are usually composed of precious metals like Au or Ag; MOFs synthesis usually requires tedious experimental procedure and ultra-dry solvent; POPs sometimes needs high temperature and oxygen pressure to aid in the light-induced oxidation; and metal oxide usually captures very narrow band of visible light.

To skirt around the mentioned disadvantages in previous systems, one should aim at: 1) using inexpensive materials to assemble the system; 2) fabricating the photocatalyst with concise procedures and easy handling methods; 3) reacting at room temperature with

* Corresponding author at: College of Chemistry and Molecular Sciences, Wuhan University, Wuhan 430072, China.
E-mail address: xianjunlang@whu.edu.cn (X. Lang).

atmosphere oxygen; 4) capturing a wide range of visible light spectrum. One recent development in the visible light photocatalytic selective oxidation of alcohols was achieved on dye-sensitized metal oxide by taking these four aims into considerations. For example, alizarin red S (ARS) [33]- or eosin Y [34]-sensitized TiO₂ were successful in performing selective oxidation of alcohols with O₂ as the oxidant; and ARS-sensitized ZnO was able to effectuate the same reactions with AgNO₃ as the oxidant [35]. However, a redox mediator of (2,2,6,6-tetramethylpiperidin-1-yl)oxyl (TEMPO) was essential for the smoothness of the oxidation reaction. The involvement of a homogeneous catalyst like TEMPO in the system makes the exclusive advantages of heterogeneous photocatalysis less apparent. Thus, more succinct heterogeneous systems should be developed without the extra engagement of TEMPO.

Particularly, two examples of visible light photocatalysis of dye-sensitized metal oxides for the selective aerobic oxidation of alcohols have been uncovered, including thionine-sensitized TiO₂-polyoxometalate (POM) [36] and flavin-sensitized ZrO₂/fluorine-doped tin oxide (FTO)-MnO₂ [37]. More recently, eosin Y-sensitized TiO₂ was extended to implement the photocatalytic aerobic oxidation of benzyl ethers to benzoates, a further indicator of the great potential of the strategy of dye-sensitized semiconductor [38]. Very interestingly, there was not a redox mediator like TEMPO engaged in these cases. Nonetheless, metal oxide complexity was increased to exploit the synergistic effect of different components of TiO₂-POM or ZrO₂/FTO-MnO₂. Simpler design in terms of metal oxides should be developed to allow for more applicable results. To this end, we want to achieve the same level of activity based on dye-sensitized metal oxide photocatalysis. Here, we report the combination of a metal-free organic dye and anatase TiO₂ to prepare a photocatalyst which in turn can animate the visible light-induced selective oxidation of a wide scope of alcohols at room temperature. Importantly, atmosphere O₂, which is a much better oxidant in terms of safety and accessibility in comparison with pure O₂, was applied as the terminal oxidant in the transformation of alcohols which is a feat that seldom be achieved in heterogeneous visible light photocatalysis.

2. Experimental section

Reagents and solvents: All the alcohols and aldehydes or ketones were procured from J&K Scientific and TCI. The solvents were supplied by Fischer Scientific and Sinopharm Chemical Reagent Co., LTD, China. Benzyl- α,α -d₂-alcohol was supplied by CDN Isotopes, Quebec, Canada. All the reagents and solvents were directly used without further purification. Anatase TiO₂ (Ishihara ST-01) used in this research was purchased from Ishihara Sangyo Kaisha, LTD., Japan. Other metal oxides like γ -Al₂O₃, SiO₂, Aeroxide TiO₂ (P25) and ZnO were supplied by Aladdin, Sigma-Aldrich, Acros Organics and Xfnano respectively.

Instrumentations and analysis conditions: The quantitative measurements of the conversions of substrates and the selectivities of products were made on a gas chromatograph equipped with a flame ionization detector (GC-FID, Agilent 7890B) using high pure N₂ as the carrier gas. The standard analysis conditions of GC-FID: injector temperature 280 °C; detector temperature 280 °C; column temperature program: 50 °C (hold 1 min) raised up to 280 °C (hold 2 min) at a rate of 20 °C/min. The samples were injected into GC-FID with an autoinjector which can warrant the accuracy of the analysis by excluding the uncontrollable factors during manual injection. The results were all obtained using a split mode with a split ratio of 30:1. An Agilent J&W DB-5 capillary column (30 m × 0.32 mm × 0.25 μm, 19,091 J-413) was selected as the column unless otherwise stated; an Agilent J&W DB-17 capillary column (30 m × 0.32 mm × 0.25 μm, 123–1732) was used for the quantitatively analysis of the products for some other substrates, including entry 6 of Table 7 and entry 1 of Table 8.

Gas chromatography-mass spectrometry (GC-MS) analysis was performed on a gas chromatograph equipped with an electron ionization mass spectrometer (Shimadzu GCMS-QP2010 Ultra) with a Restek

(Rxi®-5Sil MS) capillary column (30 m × 0.25 mm × 0.25 μm). The carrier gas for GC-MS is high pure He.

The UV-visible absorptance spectra of ARS-TiO₂ and TiO₂ samples were collected on a UV-visible spectrophotometer (Shimadzu UV 2550) equipped with a diffuse reflectance measurement accessory.

Procedure for the preparation of ARS-TiO₂: 0.075 mmol of ARS was put into a 100-mL beaker containing 30 mL of anhydrous ethanol for 10 min of ultrasonication. Then, 3 g of anatase TiO₂ (Ishihara ST-01) was put into the dispersed ARS in anhydrous ethanol for a further 10 min of ultrasonication. After that the mixture was magnetically stirred at 500 rpm for 12 h. Then ARS-TiO₂ was collected with a rotary evaporator equipped with a vacuum pump and subsequently dried at 100 °C at vacuum drying chamber for 2 h.

General procedure for the selective oxidation of alcohol: In a typical reaction, 53.8 mg of ARS-TiO₂ and 0.2 mmol of alcohol were added to 5 mL of acetonitrile (CH₃CN) in a 10 mL Pyrex vessel. Then the reaction mixture was ultrasonicated for 5 min and later stirred for 30 min in dark to reach an adsorption equilibrium. Atmosphere O₂ was directly connected to the Pyrex vessel. The reaction mixture was magnetically stirred at 1500 rpm and irradiated with 3 W green LEDs (Shenzhen Qilai Optoelectronics Science and Technology Co., LTD.) at 25 °C. After the photocatalytic reaction, the ARS-TiO₂ nanoparticles were separated from the reaction mixture by centrifugation and the products were quantitatively analysed by GC-FID using chlorobenzene as the internal standard. The structures of products were confirmed by comparison with the retention time of standard samples and further verified by GC-MS.

3. Results and discussion

We want to expand the scope of substrates and increase the applicability of dye-metal oxide photocatalysts in selective organic transformations. Therefore, the investigation on the selective aerobic oxidation of alcohols was our final target. In a first foray, we found that only 10% conversion of benzyl alcohol after 0.5 h of reaction with ambient air as the oxidant using the same ARS-TiO₂ photocatalyst for the oxidation of amines and sulfides in our previous reports. We underestimated the challenge of selective oxidation of alcohols in comparison with the oxidation of amines and sulfides. The challenges in the oxidation were supported by the fact that it was common to find reports on the transformation of N or S-containing substrates with photocatalysts like metal complexes [39] or metal-free organic dyes [40]; the reports on the oxidation of alcohols are quite exiguous. Only a few molecular photocatalysts such as flavin derivatives [41,42], sodium anthraquinone sulfonate [43] or [Ru(bpy)₃]²⁺ (bpy, bipyridyl) [44,45] were documented for the oxidation of benzylic alcohols with O₂. But flavins have to be specially modified to incur good activity and usually lack generality; and [Ru(bpy)₃]²⁺ usually needs extra additive like base or γ -Al₂O₃ to furnish product of aldehyde.

To better the photocatalytic activity for the selective oxidation of benzylic alcohols and substantially expand the scope to include aliphatic alcohols, we turned to other TiO₂ nanoparticles with different crystal phases including rutile, mixed (P25) and amorphous types to survey their activity. It was found that these ARS-TiO₂ samples provide worse conversions for the visible light photocatalytic oxidation of benzyl alcohol. Thus, we shift our attention to evaluate the influence of the amount of anatase TiO₂ on the oxidation of benzyl alcohol (Table 1). It was discovered that the amount of TiO₂ is one of the prominent factor in enhancing the conversions of benzyl alcohol without impacting the high selectivity for benzaldehyde. When the ARS was fixed at 0.67 mol% of the amount of benzyl alcohol, the decreasing of TiO₂ accounts for obvious drop in terms of conversions (from entry 1 to entry 7, Table 1). During benzyl alcohol oxidation, O₂ are believed to undergo reduction when comes into contact with the e_{cb}⁻ at the edge of conduction band. The increase of TiO₂ amount means that there is more surface area for this contact to happen, thereby leading to enhancement

Table 1

The influence of the amount of TiO_2 on the visible light-induced selective aerobic oxidation of benzyl alcohol.^a

Entry	TiO_2 [mg]		
		Conv. [%] ^b	Sel. [%] ^b
1	106.6	80	98
2	53.3	67	98
3	26.6	40	98
4	17.7	28	98
5	13.3	22	98
6	6.6	10	98
7	4.4	5	98

^a Reaction conditions: 0.2 mmol of benzyl alcohol, 1.33×10^{-3} mmol of ARS, 1 atm of air, 3 W green LED irradiation, 5 mL of CH_3CN , 0.5 h.

^b Determined by GC-FID using chlorobenzene as the internal standard, conversion of benzyl alcohol, selectivity of benzaldehyde.

in the oxidation of benzyl alcohol. The electron transfer from e_{cb}^- to O_2 is thought to be the most difficult step, whilst the ensuing reactions are consequential.

We next fetched the UV-visible absorbance spectra of TiO_2 (Fig. 1, 0) and the different ARS- TiO_2 (Fig. 1, 1–7), because it is vital to correlate visible light absorbance with their photocatalytic activity. These results provide an intriguing link between visible light absorbance and photo-induced activity. Because there is exact same quantity of ARS for the selective oxidation of same amount of benzyl alcohol, the difference in terms of TiO_2 amount can reasonably cause the variance of the ARS- TiO_2 photocatalysts in visible light absorbance converted from diffuse reflectance spectra. The pinnacle of visible light absorbance is around 500 nm and there is no apparent shift with the peaks with the change of ARS. Thus, ARS can be fully adsorbed onto TiO_2 without noticeable shifting of adsorption state at the scale of our experiment.

An appropriate light source could be a vital factor to decide whether a photochemical reaction can be applicable or not. However, this factor was often overlooked by chemists in the pursuit of improving photocatalytic processes. For TiO_2 based photocatalytic processes, Hg or Xe lamps with high wattages (100 W or 300 W) have been used as the light sources in most of the reported cases [46,47]. Even though different light sources have different undesired heating effect. The heating effect of these high-wattage light sources can be very troubling to demonstrate a true photocatalytic reaction. In the present study, light-emitting diodes (LEDs) can supply steady visible light centered around a certain wavelength with much lower heating effect during the reaction process. Therefore, it was chosen as the light source to begin the photocatalytic

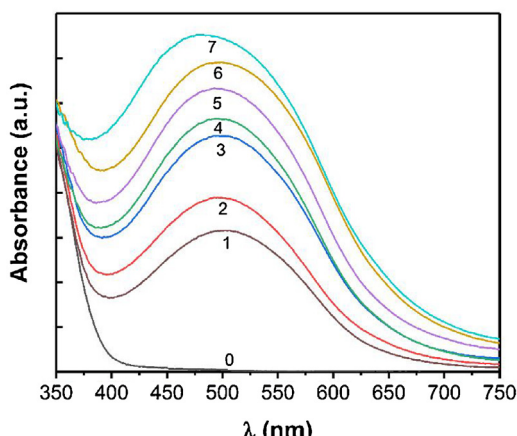


Fig. 1. UV-visible absorbance spectra of TiO_2 and ARS- TiO_2 . TiO_2 , (0); 1.33×10^{-3} mmol of ARS adsorbed onto 106.6 (1), 53.30 (2), 26.60 (3), 17.70 (4), 13.30 (5), 6.60 (6), 4.400 (7) mg of TiO_2 .

Table 2

The influence of different LED on the photocatalytic selective aerobic oxidation of benzyl alcohol.^a

Entry	LED	λ_{max} [nm]	Conv. [%] ^b	Sel. [%] ^b
1	Red	630	28	98
2	Yellow	590	48	98
3	Green	510	67	98
4	Blue	460	73	98
5	Violet	400	63	98
6	White	Continuous	65	98

^a Reaction conditions: 0.2 mmol of benzyl alcohol, 53.8 mg of ARS- TiO_2 (1.33×10^{-3} mmol of ARS), 1 atm of air, 3 W LED irradiation, 5 mL of CH_3CN , 0.5 h.

^b Determined by GC-FID using chlorobenzene as the internal standard, conversion of benzyl alcohol, selectivity of benzaldehyde.

reactions. New reactors based on LEDs have given rise to unprecedent visible light-induced reactions [48]. The influence of different 3 W LEDs (Shenzhen Qilai Optoelectronics Science and Technology Co., LTD.) on the selective aerobic oxidation of benzyl alcohol is shown in Table 2. Blue LEDs gave the best results (entry 4 vs. entries 1–3, 5 and 6 Table 2). But there was noticeable activity of visible light-induced aerobic oxidation of benzyl alcohol on anatase TiO_2 in this wavelength range even without a dye. As such, green LEDs (see supplementary data: light intensity, 0.46 mW/cm^2 when measured at 0.5 m distance; Fig. S5, light emitting spectrum) were chosen as the light source to exclude this effect for the following investigations. Furthermore, we carried out the oxidation of benzyl alcohol with 1 atm of air under $\lambda > 420 \text{ nm}$ irradiation of a 300 W Xe lamp (CEL-HXF300, Beijing China Education Au-light Co., LTD.) for comparison, 55% yield of benzaldehyde was afforded which is not as good as that of green LED irradiation (Entry 3, Table 2).

The stability of ARS- TiO_2 was proved by a survey of solvents on the visible light photocatalytic oxidation of benzyl alcohol (Table 3). Six different organic solvents were tested as the reaction medium for this oxidation reaction, delivering high selectivities of benzaldehyde in all cases (entries 1–6, Table 3). These results suggest that selectivity does not rely on solvent. In addition, it was observed no ARS was desorbed into these organic solvents. The ARS- TiO_2 nanoparticles dispersed best in CH_3CN and bestowed the best conversion of benzyl alcohol (entry 1, Table 3). There might be correlation between the slight worse dispersity of ARS- TiO_2 in these organic solvents and lower conversions of benzyl alcohol (entries 2–6, Table 3). Besides, CH_3CN is the most common solvent used for selective photocatalytic reaction mediated by TiO_2 under UV irradiation [4]. Under a milder condition of green LED irradiation, CH_3CN does not react with the photoexcited holes or electrons on TiO_2 .

Four metal-free organic dyes including ARS, eosin Y, thionine and

Table 3

The influence of solvent on the visible light-induced selective aerobic oxidation of benzyl alcohol.^a

Entry	Solvent	Conv. [%] ^b	Sel. [%] ^b
1	CH_3CN	67	98
2 ^c	BTF	31	97
3	EtOAc	20	97
4	MePh	36	99
5	DCM	31	99
6	DMF	22	96

^a Reaction conditions: 0.2 mmol of benzyl alcohol, 53.8 mg of ARS- TiO_2 (1.33×10^{-3} mmol of ARS), 1 atm of air, 3 W green LED irradiation, 5 mL of the solvent, 0.5 h. BTF, benzotrifluoride; EtOAc, ethyl acetate; MePh, methylbenzene; DCM, dichloromethane; DMF, dimethylformamide.

^b Determined by GC-FID using chlorobenzene as the internal standard, conversion of benzyl alcohol, selectivity of benzaldehyde.

^c Using biphenyl as the internal standard.

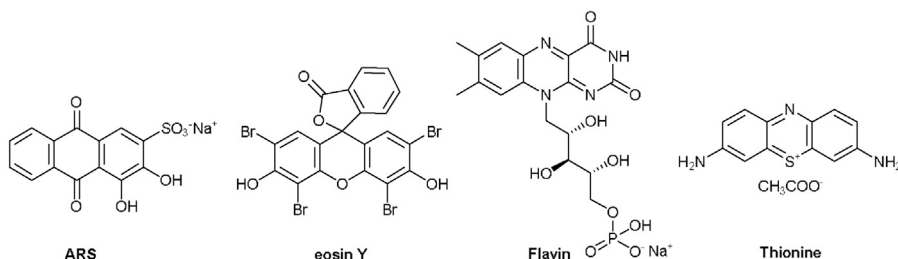


Fig. 2. Molecular structures of four metal-free organic dyes.

Table 4

The influence of different dyes and metal oxides on the visible light-induced selective aerobic oxidation of benzyl alcohol.^a

Entry	Conditions	Conv. [%] ^b	Sel. [%] ^b
1	Thionine-TiO ₂	1	98
2	Flavin-TiO ₂	34	98
3	Eosin Y-TiO ₂	50	98
4	ARS-TiO ₂	67	98
5	ARS-TiO ₂ (P25)	11	98
6	ARS-ZnO	0	–
7	ARS-γ-Al ₂ O ₃	0	–
8	ARS-SiO ₂	0	–

^a Reaction conditions: 0.2 mmol of benzyl alcohol, dye-metal oxide (1.33×10^{-3} mmol of dye; 0.67 mmol of metal oxide), 5 mL of CH₃CN, 3 W green LED irradiation, 1 atm of air, 0.5 h.

^b Determined by GC-FID using chlorobenzene as the internal standard, conversion of benzyl alcohol, selectivity of benzaldehyde.

flavin (Fig. 2) that have been proven robust enough in dye-sensitized photocatalysis for the selective oxidation of alcohols were under consideration for the optimized dye (entries 1–4, Table 4). Except thionine, the other three organic dyes can sensitize TiO₂ to animate the selective oxidation of benzyl alcohol to benzaldehyde under green LED irradiation in which ARS turns out to endow the best results. This agrees well with previous reports that ARS-TiO₂ coupled with TEMPO can engender the photocatalytic selective aerobic oxidation of other types of substrates like amines [49] and sulfides [50], indicative of the exclusive endurance and activity of ARS in sensitizing TiO₂. However, we should mention that TEMPO plays a central role to guarantee the product selectivity in both of these cases. In contrast, this role does not apply in the selective aerobic oxidation of alcohols, in which excellent selectivity was accomplished without TEMPO.

There are two interconnected parts in ARS-TiO₂, TiO₂ and ARS respectively. The choice of high specific surface area anatase TiO₂ is another reason behind the optimized result (entry 4, Table 4). Other metal oxides (see Supplementary data Table S1 and Fig. S1 for BET specific surface areas and XRD characterization) were explored in this dye-metal oxide paradigm. The supplement of anatase TiO₂ with P25 TiO₂ during the photocatalyst preparation process results in a substantial drop in the oxidation of benzyl alcohol (entry 5, Table 4). In stark contrast, another widely used semiconductor metal oxide, ZnO, cannot act the same role as that of anatase TiO₂, leading to no conversion of benzyl alcohol (entry 6, Table 4). This might be caused by the difficulty of the adsorption of ARS onto ZnO which can be visually observed that ZnO and ARS are segregated in the mixture. High specific surface area metal oxides like γ-Al₂O₃ and SiO₂ sensitized by ARS do not attribute to the oxidation of benzyl alcohol as well (entries 7 and 8, Table 4), suggesting that a reducible metal oxide is critical to the oxidation process.

After the establishment of the visible-light-induced selective oxidation of benzyl alcohol with air by ARS-sensitized TiO₂ photocatalysis,

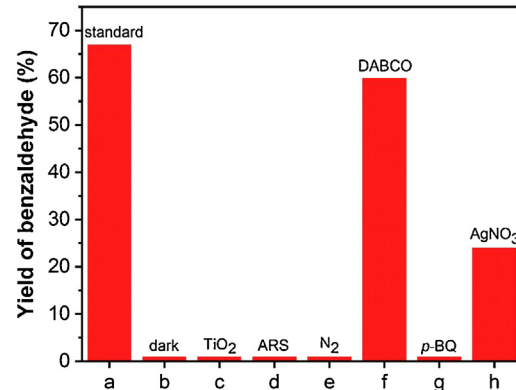
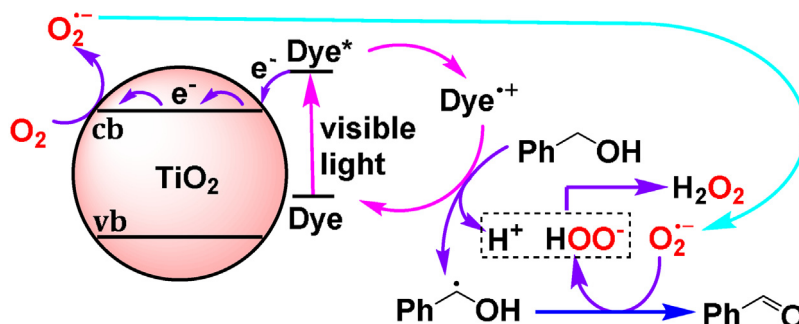


Fig. 3. The control experiments for visible light-induced selective oxidation of benzyl alcohol with air by ARS-TiO₂ photocatalysis. Reaction conditions: 0.2 mmol of benzyl alcohol, 53.8 mg of ARS-TiO₂ (1.33×10^{-3} mmol of ARS; 0.67 mmol of TiO₂), 5 mL of CH₃CN, 3 W green LED irradiation, 1 atm of air, 0.5 h. (a) standard conditions; (b) under dark conditions; (c) with 0.67 mmol of TiO₂; (d) with 1.33×10^{-3} mmol of ARS; (e) under N₂ atmosphere; (f) adding extra 0.5 equiv. of DABCO; (g) adding extra 0.1 equiv. of p-BQ; (h) adding 1 equiv. of AgNO₃.

a series of control experiments (Fig. 3) were carried out to shed more light on the mechanistic understanding of this process. One can see that the oxidation of benzyl alcohol can reach 66% of yield for benzaldehyde in 0.67 mol% of alizarin red S on the surface of TiO₂ after 0.5 h of green LED irradiation (Fig. 3a). The turnoff of LED irradiation resulted in the complete shutdown of oxidation pathway, suggesting the photocatalytic nature of the system (Fig. 3b). Moreover, neither TiO₂ nor ARS can individually expedite the transformations of benzyl alcohol (Fig. 3c and d). Therefore, the synergistic effect of TiO₂ and ARS is fundamental to the success of visible light photocatalytic design. The O₂ in air is the terminal oxidant because an exclusive N₂ atmosphere did not prompt the reaction at all (Fig. 3e). The ROS and their contribution to the final results should be determined to know the mechanistic insight on the aerobic oxidation. Thus, three additional experiments were implemented to further unravel reaction pathways (Fig. 3f–h). The 1,4-diazabicyclo[2.2.2]octane (DABCO) control result evidence that single oxygen plays a minor role in the formation of benzaldehyde (Fig. 3f); in contrast, p-benzoquinone (p-BQ) control demonstrates that O₂·⁻ plays a major role in defining the outcome (Fig. 3g). The importance of O₂·⁻ was reinforced by that adding 1 equiv. of AgNO₃ as a competitive electron acceptor to O₂ triggered marked decrease to 23% yield of benzaldehyde (Fig. 3h). Furthermore, the amounts of AgNO₃ were varied to 0.5 equiv. and 2 equiv. which consequently led the yields of benzaldehyde to 37% and 20% respectively. Hence, one can conclude that AgNO₃ cannot completely switch off the involvement of O₂·⁻ in contributing to the formation of benzaldehyde. Furthermore, the presence of O₂·⁻ trapping experiment with 5,5-dimethyl-1-pyrroline N-oxide (DMPO) was also traced by ESR signal (see supplementary data Fig. S2) which is in good agreement with previous report [51].

We tentatively propose a reaction mechanism in Scheme 1, based on the results of the above-mentioned control experiments. The adsorption of ARS onto the surface of TiO₂ underpins all the subsequent



Scheme 1. The proposed mechanism for visible light-induced selective oxidation of benzyl alcohol with air by dye-sensitized TiO_2 photocatalysis.

photocatalytic steps [52], occurring during the preparation of ARS- TiO_2 photocatalyst stage. Under visible light irradiation, the ARS adsorbed on the surface of TiO_2 will be excited to its excited state ARS^* whose quenching results in the injection of electron to the conduction band (cb) of TiO_2 and generation of ARS radical cations, ARS^+ . Benzyl alcohol captures ARS^+ to restore to its ground state, the adsorbed ARS which in turn transforms itself to benzyl alcohol radical and H^+ . The valence band (vb) was completely avoided during the reaction process. Next, conduction band e_{cb}^- reduces O_2 to $\text{O}_2^{\cdot-}$. Superoxide $\text{O}_2^{\cdot-}$ interacts with benzyl alcohol radical to afford benzaldehyde product and $\text{HOO}^{\cdot-}$. The interaction of H^+ and $\text{HOO}^{\cdot-}$ results in the formation of H_2O_2 , qualitatively confirmed by the colour change of a potassium iodide-starch test paper in the CH_3CN solution after the reaction. Thus, H_2O_2 was the side product of the selective aerobic oxidation process. Superoxide $\text{O}_2^{\cdot-}$, observed by ESR, was critical in directing the oxidation product formation, supported by both p-BQ quenching $\text{O}_2^{\cdot-}$ and AgNO_3 accepting e_{cb}^- control experiments.

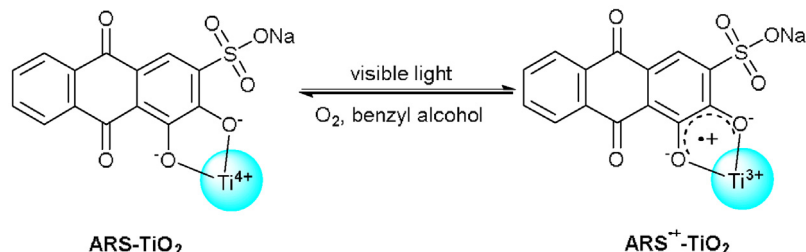
The binding and interaction of organic dyes and TiO_2 is crucial to the electron injection to the conduction band of TiO_2 [53]. In particular, the adsorption of catechol onto TiO_2 has been well established as a model system for the strong interaction between a class of dyes containing catechol motifs and metal oxide [54]. Under visible light irradiation, the direct electron injection from the ground state of ARS to the conduction band of TiO_2 by a bidentate mononuclear cheating linkage (Scheme 2). [55] In addition, this linkage resonance makes sure that ARS can be adsorbed at the Brønsted acid sites of TiO_2 under electron transfer state. We believed that this linkage is very helpful to convey a very high photocatalytic activity for the visible light-induced oxidation of benzyl alcohol. Under ideal conditions, ARS should be kept intact on the surface of TiO_2 . In a realistic scenario, the chemically adsorbed ARS was partially degraded at the interfaces without entering into the solution of CH_3CN to contaminate the product. Therefore, no extra effort was required to purify the product.

With these insights in hand, we next performed kinetics studies on the visible light-induced selective oxidation of benzyl alcohol with air by ARS- TiO_2 (Fig. 4a). Meanwhile, the selective oxidation of benzyl- $\alpha,\alpha\text{-d}_2$ alcohol with air was also carried out (Fig. 4b) for a comparison. After obtaining the relationship between the yield of benzaldehyde against time, we further analyzed the kinetics data to establish the reaction constant (Fig. 4c), which can be roughly recognized as pseudo

first-order reaction with a reaction constant as $k_H = 2.77 \times 10^{-2} \text{ min}^{-1}$. The same reaction pattern follows for the selective oxidation of benzyl- $\alpha,\alpha\text{-d}_2$ alcohol (Fig. 4b), with a reaction constant as $k_D = 1.24 \times 10^{-2} \text{ min}^{-1}$ (Fig. 4d). The kinetics isotope effect (KIE) value is $k_H/k_D = 2.23$. The KIE value of this range suggests it belongs to primary KIE and the activation of $C_\alpha\text{-H}$ in benzyl alcohol is the rate determining step.

To further verify the reaction follows pseudo first-order reaction kinetics rather than first-order reaction kinetics, we studied the influence of the initial concentration of benzyl alcohol on the reaction results (Table 5) by simply changing the amount of CH_3CN . One should observe that the conversions decreased with the decrease of initial concentration of benzyl alcohol while maintaining the concentration of ARS- TiO_2 photocatalyst constant for first-order reaction kinetics. In contrast, it was found that the conversions decreased with the increase of initial concentration of benzyl alcohol under the same the concentration of ARS- TiO_2 photocatalyst (from entry 1 to entry 5, Table 5). This is a heterogeneous catalytic system. One might doubt the same the concentration of ARS- TiO_2 photocatalyst is not very relevant. Thus, we fixed the surface area of ARS- TiO_2 photocatalyst and found that the increase of the initial concentration of benzyl alcohol does not impact the conversion apparently (from entry 5 to entry 9, Table 5). Therefore, one can conclude that pseudo first-order reaction kinetics is a more plausible proposition for the visible light-induced oxidation of alcohols by ARS- TiO_2 photocatalysis.

To know the generality of this strategy of visible light-induced selective aerobic oxidation by ARS- TiO_2 photocatalysis (see supplementary data Figs. S3 and S4 for XRD and TEM characterizations of TiO_2 and ARS- TiO_2 ; BET specific surface area of TiO_2 and ARS- TiO_2 , 256.7 and $233.4 \text{ m}^2/\text{g}$), we first expand the scope to benzyl alcohol and its para-substituted derivatives (Table 6). For all these alcohol substrates, high selectivities for corresponding aldehydes were furnished with 1 atm of air as the terminal oxidant within 2 h of reaction time. Over-oxidation of benzylic alcohols to corresponding carboxylic acids was not observed. During the first 0.5 h of reaction time, 67% conversion of benzyl alcohol can be obtained, but 2 h or reaction time was needed for 87% conversion of benzyl alcohol (entry 1, Table 6). When we raised the quantity of benzyl alcohol to 0.4 mmol, only 45% conversion of benzyl alcohol was achieved (entry 2, Table 6), about the same absolute quantity of benzyl alcohol as 0.2 mmol of benzyl alcohol (entry 1,



Scheme 2. The adsorption and visible light-induced electron transfer between ARS and TiO_2 .

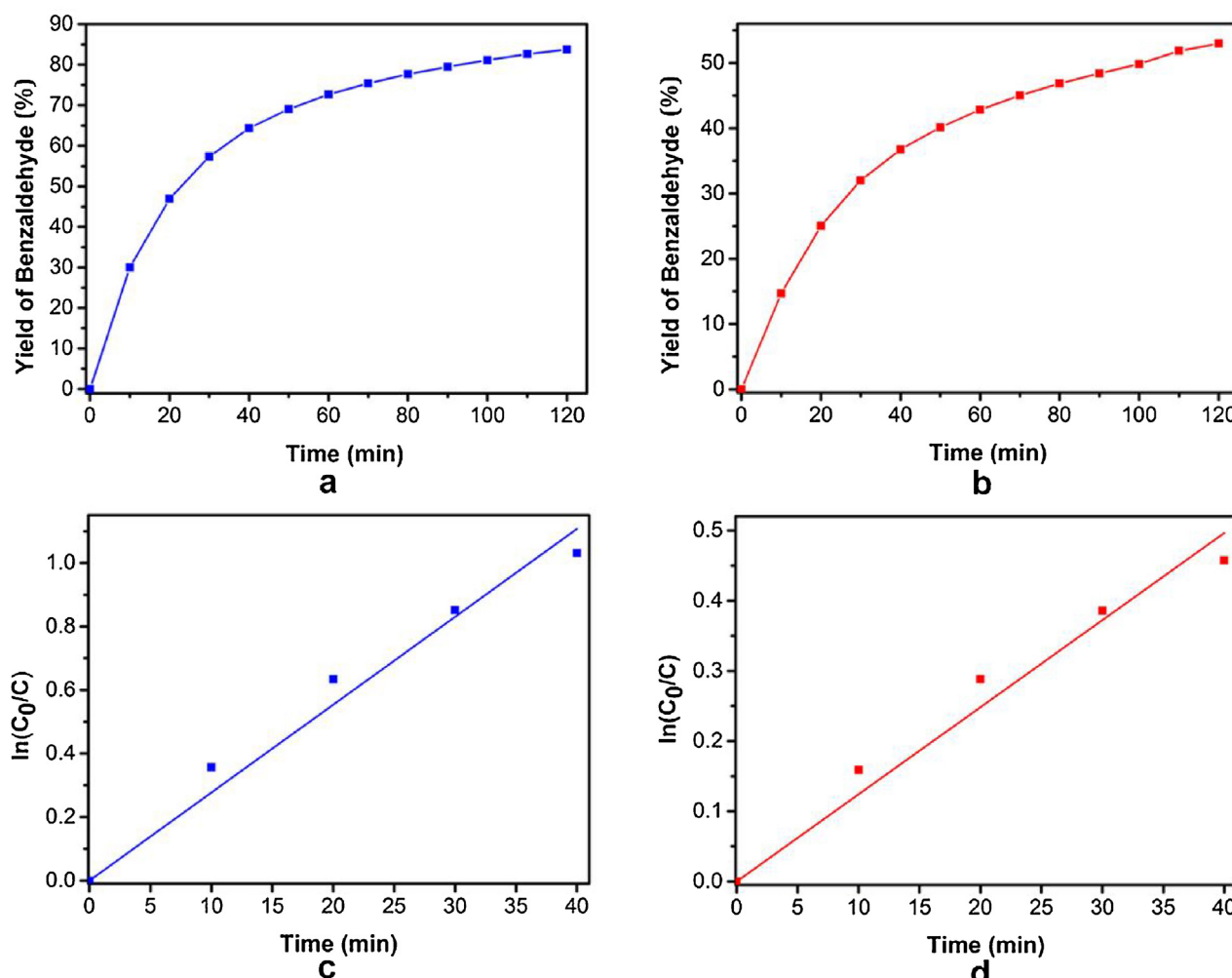


Fig. 4. The reaction kinetics for the visible light-induced selective oxidation of benzyl alcohol with air. **a**, The yield of benzaldehyde against the reaction time for the oxidation of benzyl alcohol; **b**, the yield of benzaldehyde- α -d₁ against reaction time for the oxidation of benzyl- α,α -d₂ alcohol; **c**, linear fit of $\ln(C_0/C)$ against time for the oxidation of benzyl alcohol; **d**, linear fit of $\ln(C_0/C)$ against time for the oxidation of benzyl- α,α -d₂ alcohol. C_0 , the initial concentration of alcohol; C , the concentration of alcohol. Reaction conditions: 0.2 mmol of benzyl alcohol, 53.8 mg of ARS-TiO₂ (1.33×10^{-3} mmol of ARS), 3 W green LED irradiation, 1 atm of air (For interpretation of the references to colour in this figure legend, the reader is referred to the web version of this article).

Table 5

The influence of the initial concentration of benzyl alcohol on the selective aerobic oxidation by ARS-TiO₂ photocatalysis.^a

Entry	ARS-TiO ₂ [mg]	CH ₃ CN[mL]	C ₀ [M]	Conv.[%] ^b	Sel.[%] ^b
1	10.8	1	0.200	14	98
2	21.5	2	0.100	31	98
3	32.3	3	0.067	40	98
4	43.0	4	0.050	51	98
5	53.8	5	0.020	67	98
6	53.8	4	0.050	60	98
7	53.8	3	0.067	60	98
8	53.8	2	0.100	59	98
9	53.8	1	0.200	52	98

^a Reaction conditions: 0.2 mmol of benzyl alcohol, ARS-TiO₂, 1 atm of air, 3 W green LED irradiation, 0.5 h.

^b Determined by GC-FID using chlorobenzene as the internal standard, conversion of benzyl alcohol, selectivity of benzaldehyde.

Table 6. The recycle of the ARS-TiO₂ photocatalyst cannot be directly obtained due to the partial degradation of ARS attacked by ROS generated during the photocatalytic process. As such, the visible light activity faded away. However, after collecting the spent photocatalyst, we add new ARS suspension in CH₃CN and repeat the ARS-TiO₂

preparation process, restoring the conversion of benzyl alcohol to 90% in 2 h under green LED irradiation. In this investigation with fixed time, the conversions for the para-substituted benzyl alcohol almost follows the order that the electron donating groups have better conversions than that of electron withdrawing groups (entries 3–5 vs. entries 6–8, 10–12, **Table 6**). The conversion for the I-para-substituted benzyl alcohol was abnormally high (entry 9, **Table 6**); F-para-substituted benzyl alcohol was abnormally low (entry 6, **Table 6**). The reason for these phenomena is not quite clear at this stage, leaving much room for further investigation.

The scope of this visible light-induced protocol for oxidation of alcohols could be further expanded to other aromatic alcohols (**Table 7**). Benzyl alcohols with ortho-, meta-substituted MeO group can be subject to the conditions with moderate or good conversions of alcohols (entries 1 and 2, **Table 7**). This protocol is also very efficient in the selective oxidation of secondary benzyl alcohols with good conversions and excellent selectivities (entries 3–6, **Table 7**). Installing OH group into the phenyl ring of benzyl alcohol resulted in low conversion and very unacceptable selectivity (entry 7, **Table 7**). For the oxidation of alcohol like this, protecting group is needed to ensure the stability in the OH position. Heteroatom-containing aromatic alcohols can undergo favorable aldehydes formation but with low conversions (entries 8 and 9, **Table 7**). When furfuryl alcohol was subjected to the reaction

Table 6

Visible light-induced selective oxidation of benzyl alcohol and its derivatives to aldehydes with air by ARS-TiO₂ photocatalysis.^a

Entry	Substrate	Product	Conv. [%] ^b	Sel. [%] ^b
1			87	98
2 ^[c]			45	98
3			91	98
4			92	98
5			87	98
6			68	98
7			77	98
8			80	98
9			100	98
10			71	97
11			65	98
12			64	99

^a Reaction conditions: 0.2 mmol of alcohol, 53.8 mg of ARS-TiO₂ (1.33×10^{-3} mmol of ARS), 1 atm of air, 3 W green LED irradiation, 5 mL of CH₃CN, 2 h.

^b Determined by GC-FID using chlorobenzene as the internal standard, conversion of alcohol, selectivity of the corresponding aldehyde. ^c 0.4 mmol of benzyl alcohol.

Table 7

Visible light-induced selective oxidation of other aromatic alcohols to aldehydes or ketones with air by ARS-TiO₂ photocatalysis.^a

Entry	Substrate	Product	Conv. [%] ^b	Sel. [%] ^b
1			64	98
2			80	98
3			87	96
4			88	95
5			84	97
6			68	98
7			49	24
8			36	89
9			51	88
10			56	35

^a Reaction conditions: 0.2 mmol of alcohol, 53.8 mg of ARS-TiO₂ (1.33×10^{-3} mmol of ARS), 1 atm of air, 3 W green LED irradiation, 5 mL of CH₃CN, 2 h.

^b Determined by GC-FID using chlorobenzene as the internal standard, conversion of alcohol, selectivity of the corresponding aldehyde or ketone.

conditions, very low selectivity of furfuryl aldehyde, a common model compound for conversions of biomass [56], was afforded (entry 10, Table 7). Thus, if one wants to transfer this protocol to biomass conversion, further improving the photocatalyst and/or engineering the process is required.

Aliphatic and allylic alcohols are the most challenging substrates

Table 8

Visible light-induced selective oxidation of other representative alcohols to aldehydes or ketones with air by ARS-TiO₂ photocatalyst.^a

Entry	Substrate	Product	Conv. [%] ^b	Sel. [%] ^b
1			38	97
2			18	78
3			11	87
4			62	69
5			62	56

^a Reaction conditions: 0.2 mmol of alcohol, 53.8 mg of ARS-TiO₂ (1.33×10^{-3} mmol of ARS), 1 atm of air, 3 W green LED irradiation, 5 mL of CH₃CN, 2 h.

^b Determined by GC-FID using chlorobenzene as the internal standard, conversion of alcohol, selectivity of the corresponding aldehyde or ketone.

during the photocatalytic oxidation process. Therefore, we continue to widen the use of this protocol to implement the oxidation of these types of substrates (Table 8). To our surprise, the selectivities for the selective oxidation with aliphatic primary and secondary alcohols were quite good (entries 1–3, Table 8), further suggesting the generality of this protocol. However, the conversions of alcohols need to be furthered for potential application. In the case for the oxidation of allylic alcohols, better conversions but lower selectivities were obtained (entries 4 and 5, Table 8) in comparison with the aliphatic ones (entries 1–3, Table 8). This is predictable outcome because that O₂^{·-} is the central ROS in affording the aldehydes as suggested in Scheme 1. The motifs of unsaturated C=C double bonds in allylic alcohols is susceptible to be attacked by O₂^{·-}, leading to undesired oxidation products.

4. Conclusion

In summary, we have provided a compelling use of dye-sensitized metal oxide strategy to access chemically challenging reactions like the oxidation of alcohols with atmosphere O₂ as a terminal oxidant. The result proved that a common textile dye like ARS can be directly used as a photocatalyst for selective oxidation reaction under ambient conditions, provided that the surface of anatase TiO₂ can be a platform. This research is hitherto one of the first use of dye-sensitized TiO₂ to directly regulate the formation of aldehydes by photocatalytic selective aerobic oxidation of alcohols. Even though some experimental work has been carried out to get a preliminary understanding of the reaction process, much mechanism remains unclear which accordingly needs further effort to identify the elaborated reaction pathways. The related work is still underway in our group.

Acknowledgements

This research was financially supported by the National Natural Science Foundation of China (grants 21503086 and 21773173), 111 project (B12015) and the start-up fund of Wuhan University.

Appendix A. Supplementary data

Supplementary material related to this article can be found, in the online version, at doi:<https://doi.org/10.1016/j.apcatb.2018.03.043>.

References

- [1] T. Kamegawa, S. Matsuura, H. Seto, H. Yamashita, Angew. Chem. Int. Ed. 52 (2013) 916–919.
- [2] C.C. Chen, W.H. Ma, J.C. Zhao, Chem. Soc. Rev. 39 (2010) 4206–4219.
- [3] J.W. Zhou, M. Zhang, Y.F. Zhu, Phys. Chem. Chem. Phys. 17 (2015) 3647–3652.
- [4] X.J. Lang, W.H. Ma, C.C. Chen, H.W. Ji, J.C. Zhao, Acc. Chem. Res. 47 (2014)

- 355–363.
- [5] J.H. Kou, C.H. Lu, J. Wang, Y.K. Chen, Z.Z. Xu, R.S. Varma, *Chem. Rev.* 117 (2017) 1445–1514.
- [6] G. Palmisano, E. García-López, G. Marci, V. Loddo, S. Yurdakal, V. Augugliaro, L. Palmisano, *Chem. Commun.* 46 (2010) 7074–7089.
- [7] H. Kisch, *Acc. Chem. Res.* 50 (2017) 1002–1010.
- [8] X.J. Lang, X.D. Chen, J.C. Zhao, *Chem. Soc. Rev.* 43 (2014) 473–486.
- [9] Q. Xiao, E. Jaatinen, H.Y. Zhu, *Chem. Asian J.* 9 (2014) 3046–3064.
- [10] L. Palmisano, V. Augugliaro, M. Bellardito, A. Di Paola, E.G. Lopez, V. Loddo, G. Marci, G. Palmisano, S. Yurdakal, *ChemSusChem* 4 (2011) 1431–1438.
- [11] J.C. Colmenares, R. Luque, *Chem. Soc. Rev.* 43 (2014) 765–778.
- [12] S. Yurdakal, G. Palmisano, V. Loddo, V. Augugliaro, L. Palmisano, *J. Am. Chem. Soc.* 130 (2008) 1568–1569.
- [13] Z.R. Tang, X. Yin, Y.H. Zhang, Y.J. Xu, *RSC Adv.* 3 (2013) 5956–5965.
- [14] T. Shishido, T. Miyatake, K. Teramura, Y. Hitomi, H. Yamashita, T. Tanaka, *J. Phys. Chem. C* 113 (2009) 18713–18718.
- [15] D. Tsukamoto, M. Ikeda, Y. Shiraishi, T. Hara, N. Ichikuni, S. Tanaka, T. Hirai, *Chem. Eur. J.* 17 (2011) 9816–9824.
- [16] M. Qamar, R.B. Elsayed, K.R. Alhooshani, M.I. Ahmed, D.W. Bahemann, *ACS Appl. Mater. Interfaces* 7 (2015) 1257–1269.
- [17] B. Zhang, J. Li, Y.Y. Gao, R.F. Chong, Z.L. Wang, L. Guo, X.W. Zhang, C. Li, *J. Catal.* 345 (2017) 96–103.
- [18] A. Abd-Elaal, F. Parrino, R. Ciriminna, V. Loddo, L. Palmisano, M. Pagliaro, *ChemistryOpen* 4 (2015) 779–785.
- [19] X.G. Zhang, X.B. Ke, H.Y. Zhu, *Chem. Eur. J.* 18 (2012) 8048–8056.
- [20] Y. Sugano, Y. Shiraishi, D. Tsukamoto, S. Ichikawa, S. Tanaka, T. Hirai, *Angew. Chem. Int. Ed.* 52 (2013) 5295–5299.
- [21] Y. Chen, Y.N. Wang, W.Z. Li, Q. Yang, Q.D. Hou, L.H. Wei, L. Liu, F. Huang, M.T. Ju, *Appl. Catal. B* 210 (2017) 352–367.
- [22] X.Y. Wu, E. Jaatinen, S. Sarina, H.Y. Zhu, *J. Phys. D: Appl. Phys.* 50 (2017) 283001.
- [23] S. Yuan, T.F. Liu, D.W. Feng, J. Tian, K.C. Wang, J.S. Qin, Q. Zhang, Y.P. Chen, M. Bosch, L.F. Zou, S.J. Teat, S.J. Dalgararno, H.C. Zhou, *Chem. Sci.* 6 (2015) 3926–3930.
- [24] Y.Z. Chen, Z.U. Wang, H.W. Wang, J.L. Lu, S.H. Yu, H.L. Jiang, *J. Am. Chem. Soc.* 139 (2017) 2035–2044.
- [25] F.Z. Su, S.C. Mathew, G. Lipner, X.Z. Fu, M. Antonietti, S. Blechert, X.C. Wang, *J. Am. Chem. Soc.* 132 (2010) 16299–16301.
- [26] W. Huang, B.C. Ma, H. Lu, R. Li, L. Wang, K. Landfester, K.A.I. Zhang, *ACS Catal.* 7 (2017) 5438–5442.
- [27] Y.H. Zhang, Y.J. Xu, *RSC Adv.* 4 (2014) 2904–2910.
- [28] K.Q. Jing, J.H. Xiong, N. Qin, Y.J. Song, L.Y. Li, Y. Yu, S.J. Liang, L. Wu, *Chem. Commun.* 53 (2017) 8604–8607.
- [29] T.F. Li, T. Kasahara, J.F. He, K.E. Dettelbach, G.M. Sammis, C.P. Berlinguet, *Nat. Commun.* 8 (2017) 390.
- [30] C.A. Unsworth, B. Coulson, V. Chechik, R.E. Douthwaite, *J. Catal.* 354 (2017) 152–159.
- [31] S. Higashimoto, N. Kitao, N. Yoshida, T. Sakura, M. Azuma, H. Ohue, Y. Sakata, *J. Catal.* 266 (2009) 279–285.
- [32] L.H. Yu, Y.M. Lin, D.Z. Li, *Appl. Catal. B* 216 (2017) 88–94.
- [33] M. Zhang, C.C. Chen, W.H. Ma, J.C. Zhao, *Angew. Chem. Int. Ed.* 47 (2008) 9730–9733.
- [34] Y.C. Zhang, Z. Wang, X.J. Lang, *Catal. Sci. Technol.* 7 (2017) 4955–4963.
- [35] V. Jeena, R.S. Robinson, *Chem. Commun.* 48 (2012) 299–301.
- [36] X. Yang, H. Zhao, J.F. Feng, Y.M. Chen, S.Y. Gao, R. Cao, *J. Catal.* 351 (2017) 59–66.
- [37] P. Dongare, I. MacKenzie, D.G. Wang, D.A. Nicewicz, T.J. Meyer, *Proc. Natl. Acad. Sci. U. S. A.* 114 (2017) 9279–9283.
- [38] L. Ren, M.M. Yang, C.H. Tung, L.Z. Wu, H. Cong, *ACS Catal.* 7 (2017) 8134–8138.
- [39] D.M. Schultz, T.P. Yoon, *Science* 343 (2014) 1239176.
- [40] D. Ravelli, M. Fagnoni, A. Albini, *Chem. Soc. Rev.* 42 (2013) 97–113.
- [41] U. Megerle, M. Wenninger, R.-J. Kutta, R. Lechner, B. König, B. Dick, E. Riedle, *Phys. Chem. Chem. Phys.* 13 (2011) 8869–8880.
- [42] K.A. Korvinson, G.N. Hargenrader, J. Stevanovic, Y. Xie, J. Joseph, V. Maslak, C.M. Hadad, K.D. Glusac, *J. Phys. Chem. A* 120 (2016) 7294–7300.
- [43] W.Y. Zhang, J. Gacs, I.W.C.E. Arends, F. Hollmann, *ChemCatChem* 9 (2017) 3821–3826.
- [44] W.R. Leow, W.K.H. Ng, T. Peng, X.F. Liu, B. Li, W.X. Shi, Y. Lum, X.T. Wang, X.J. Lang, S.Z. Li, N. Mathews, J.W. Ager, T.C. Sum, H. Hirao, X.D. Chen, *J. Am. Chem. Soc.* 139 (2017) 269–276.
- [45] D.W. Liu, H.X. Zhou, X.Y. Gu, X.Q. Shen, P.X. Li, *Chin. J. Chem.* 32 (2014) 117–122.
- [46] X.J. Lang, H.W. Ji, C.C. Chen, W.H. Ma, J.C. Zhao, *Angew. Chem. Int. Ed.* 50 (2011) 3934–3937.
- [47] X.J. Lang, W. Hao, W.R. Leow, S.Z. Li, J.C. Zhao, X.D. Chen, *Chem. Sci.* 6 (2015) 5000–5005.
- [48] D.K. Kim, V.M. Dong, *ACS Cent. Sci.* 3 (2017) 526–527.
- [49] Z. Wang, X.J. Lang, *Appl. Catal. B* 224 (2018) 404–409.
- [50] X.J. Lang, J.C. Zhao, X.D. Chen, *Angew. Chem. Int. Ed.* 55 (2016) 4697–4700.
- [51] Y.Y. Wang, W.J. Yang, X.J. Chen, J. Wang, Y.F. Zhu, *Appl. Catal. B* 220 (2018) 337–347.
- [52] Y.D. Iorio, E.S. Román, M.I. Litter, M.A. Grela, *J. Phys. Chem. C* 112 (2008) 16532–16538.
- [53] Y. Ooyama, K. Furue, T. Enoki, M. Kanda, Y. Adachi, J. Ohshita, *Phys. Chem. Chem. Phys.* 18 (2016) 30662–30676.
- [54] D. Finkelstein-Shapiro, S.K. Davidowski, P.B. Lee, C.C. Guo, G.P. Holland, T. Rajh, K.A. Gray, J.L. Yarger, M. Calatayud, *J. Phys. Chem. C* 120 (2016) 23625–23630.
- [55] W. Ji, Y. Wang, I. Tanabe, X.X. Han, B. Zhao, Y. Ozaki, *Chem. Sci.* 6 (2015) 342–348.
- [56] T. Yang, Y.H. Zhou, S.Z. Zhu, H. Pan, Y.B. Huang, *ChemSusChem* 10 (2017) 4066–4079.